

1 Protective Structures with Waiting Links 2 and Their Damage Evolution

3 ANDREJ CHERKAEV¹ and LIYA ZHORNITSKAYA²

4 ¹*Bradenburg University of Technology, Cottbus, Germany;* ²*Department of Mathematics, University
 5 of Utah, Salt Lake City, UT 84112, USA*

6 (Received: 19 May 2004; accepted in revised form: 19 May 2004)

7 **Abstract.** The paper is concerned with simulation of the damage spread in protective structures
 8 with “waiting links.” These highly nonlinear structures switch their elastic properties whenever the
 9 elongation of a link exceeds a critical value; they are stable against dynamic impacts due to their
 10 morphology. Waiting link structures are able to spread “partial damage” through a large region,
 11 thereby dissipating the energy of the impact. We simulate various structures with waiting links and
 12 compare their characteristics with conventional designs. The figures show the damage propagation in
 13 several two-dimensional structures.

14 **Keywords:** dynamics of damage, failure, structures

15 **1. Introduction**

16 **1.1. WAITING ELEMENTS AND SPREAD OF DAMAGE**

17 This paper describes protective structures that exhibit an unusually high dissipation
 18 if they are subject to a concentrated (ballistic) impact. Under this impact, the struc-
 19 ture experiences very large forces applied during a short time. The kinetic energy
 20 of the projectile must be absorbed in the structure. We want to find a structure
 21 that absorbs maximal kinetic energy of the projectile without rupture or breakage.
 22 Here, we consider dilute structures. Specifically, we define the structure as an as-
 23 sembly (network) of rods connected in knots. The structure may be submerged into
 24 a viscous substance.

25 While theoretically a material can absorb energy until it melts, real structures are
 26 destroyed by a tiny fraction of this energy due to material instabilities and an uneven
 27 distribution of the stresses throughout the structure. Therefore, we increase the sta-
 28 bility of the process of damage by a special morphology of the structural elements.

29 The increase of the stability is achieved due to special structural elements used
 30 for the assembly: the so-called “waiting links”. These elements contain parts that
 31 are initially inactive and start to resist only when the strain is large enough; they lead
 32 to large but stable pseudo-plastic strains; structures distribute the strain over a large
 33 area, in contrast to unstructured solid materials where the strain is concentrated
 34 near the zone of an impact. Similar structures are considered in [1, 4, 6, 9, 10]. The
 35 continuum models are discussed in [2]; experimental study is performed in [8].

In this paper we introduce a model for dynamic failure of links made from brittle-elastic materials, discuss the dynamics of networks of waiting links, a model of the penetrating projectile and the criteria of resistance of deteriorating structures. We simulate the damage spread in the lattices and optimize their parameters. The figures demonstrate elastic waves and waves of damage in the lattices and visualize the damage evolution.

2. Equations and Algorithms

2.1. BRITTLE-ELASTIC BAR

Consider a stretched rod from a homogeneous elastic-brittle material. If slowly loaded, this material behaves as a linear elastic one, unless the length z reaches a critical value z_f , and fails (becomes damaged) after this. The critical value z_f is proportional to the length L of the rod at equilibrium

$$z_f = L(1 + \epsilon_f) \quad (1)$$

where the critical strain ϵ_f is a material's property. The static force F_{static} in such a rod depends on its length z as

$$F_{\text{static}}(z) = \begin{cases} ks(z/L - 1) & \text{if } z < z_f \\ 0 & \text{if } z \geq z_f \end{cases} \quad (2)$$

where k is elastic modulus and s is the cross-section of the rod.

2.1.1. Dynamic Model of Damage Increase

We are interested to model the dynamics of damageable rods; therefore we need to expand the model of brittle material adding the assumption of the dynamics of the failure. We assume that the force F in such a rod depends on its length z and on damage parameter c :

$$F(z, c) = ks(1 - c)(z/L - 1). \quad (3)$$

The damage parameter c is equal to zero if the rod is not damaged and is equal to one if the rod is destroyed; in the last case the force obviously is zero. Development of the damage is described as the increase of the damage parameter $c(z, t)$ from zero to one. The damage parameter equals zero in the beginning of the deformation and it remains zero until a moment when the elongation exceeds a critical value; it can only increase in time. This parameter depends on the history of the deformation of the sample.

63 We suggest to describe the increase of the damage parameter by the differential
 64 equation

$$\frac{dc(z, t)}{dt} = \begin{cases} v_d & \text{if } z \geq z_f \text{ and } c < 1 \\ 0 & \text{otherwise} \end{cases}, \quad c(0) = 0 \quad (4)$$

65 where z_f is the maximal elongation that the element can sustain without being
 66 damaged, and v_d is the speed of damage. This equation states that the damage
 67 increases in the instances when the elongation exceeds the limit z_f ; the increase of
 68 damage stops if the element is already completely damaged. The speed v_d can be
 69 chosen as large as needed.

70 *Remark 1.* The damage can also be modeled by a discontinuous function c_H that
 71 is equal to zero if the element is undamaged and equal to one if it is disrupt:

$$c_H(z, t) = \lim_{v_d \rightarrow \infty} c(z, t).$$

72 Use of a continuously varying damage parameter (4) instead of a discontinuous one
 73 increases stability of the computational scheme.

74 *Remark 2.* One can argue about the behavior of the rod with an intermediate
 75 value of the damage parameter. We do not think that these states need a special
 76 justification: they simply express the fact that the stiffness rapidly deteriorates to
 77 zero when the sample is over-strained. We notice that in the simulations presented
 78 here the time of transition from undamaged to damaged state is short.

79 2.2. WAITING LINKS

80 Here we introduce special structural elements – waiting links – that several times
 81 increase the resistivity of the structure due to their morphology. These elements
 82 and their quasistatic behavior are described in [1]. The link is an assembly of two
 83 elastic-brittle rods, lengths L and Δ ($\Delta > L$) joined by their ends (see Figure 1,
 84 left). The longer bar is initially slightly curved to fit. When the link is stretched by a
 85 slowly increasing external elongation, only the shortest rod resists in the beginning.
 86 If the elongation exceeds a critical value, this rod breaks at some place between
 87 two knots. The next (longer) rod then assumes the load replacing the broken one.

88 Assume that a unit volume of material is used for both rods. This amount is
 89 divided between the shorter and longer rod: the amount α is used for the shorter
 90 (first) rod and the amount $1 - \alpha$ is used for the longer (second) one. The cross-
 91 sections s_1 and s_2 of rods are:

$$s_1(\alpha) = \frac{\alpha}{L} \quad \text{and} \quad s_2(\alpha) = \frac{1 - \alpha}{\Delta}, \quad (5)$$

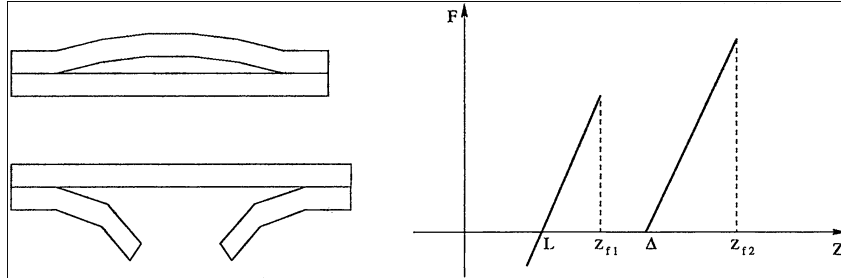


Figure 1. Left above: The waiting link in the initial state. Left below: The waiting link after the first rod is broken. Right: The force versus length dependence for a monotone elongation.

so that

92

$$s_1(\alpha)L + s_2(\alpha)\Delta = \text{volume} = 1$$

The force versus elongation dependence in the shorter rod is:

93

$$F_1(z) = ks_1(\alpha) \left(\frac{z}{L} - \right) (1 - c_1) \quad (6)$$

where $c_1 = c_1(z, t)$ is the damage parameter for this rod; it satisfies the equation similar to (4)

94

95

$$\frac{dc_1(z, t)}{dt} = \begin{cases} v_d & \text{if } z \geq z_{f1} \text{ and } c_1(z, t) < 1 \\ 0 & \text{otherwise} \end{cases} \quad c_1(z, 0) = 0 \quad (7)$$

where $z_{f1} = L(1 + \epsilon_f)$.

96

The longer rod starts to resist when the elongation z is large enough to straighten this rod. After the rod is straight, the force versus elongation dependence is similar to that for the shorter rod:

97

98

99

$$F_2(z) = \begin{cases} ks_2(\alpha) \left(\frac{z}{\Delta} - 1 \right) (1 - c_2), & \text{if } z \geq \Delta \\ 0, & \text{if } z < \Delta \end{cases} \quad . \quad (8)$$

Here F_2 is the resistance force and $c_2 = c_2(z, t)$ is the damage parameter for the second rod:

100

101

$$\frac{dc_2(z, t)}{dt} = \begin{cases} v_d & \text{if } z \geq z_{f2} \text{ and } c_2(z, t) < 1 \\ 0 & \text{otherwise} \end{cases} \quad c_2(z, 0) = 0 \quad (9)$$

Those equations are similar to (6), (7), where the cross-section $s_1(\alpha)$ is replaced by $s_2(\alpha)$ and the critical elongation z_{f1} by $z_{f2} = \Delta(1 + \epsilon_f)$. The difference between the two rods is that the longer (slack) rod starts to resist only when the elongation is large enough.

102

103

104

105

106 The total resistance force $F(z)$ in the waiting link is the sum of $F_1(z)$ and $F_2(z)$:

$$F(z) = F_1(z) + F_2(z). \quad (10)$$

107 The graph of this force versus elongation dependence for the monotone external
108 elongation is shown in Figure 1 (right) where the damage parameters jump from
109 zero to one at the critical point z_{f_1} .

110 One observes that the constitutive relation $F(z)$ is nonmonotone. Therefore one
111 should expect that the dynamics of an assembly of such elements is characterized
112 by abrupt motions and waves (similar systems but without damage parameter were
113 investigated in [5, 6]).

114 2.3. DYNAMICS

115 It is assumed that the inertial masses m_i are concentrated in the knots joined by the
116 inertialess waiting links (nonlinear springs), therefore the dynamics of the structure
117 is described by ordinary differential equations of motion of the knots. We assume
118 that the links are elastic-brittle, as it is described above. Additionally, we assume that
119 the space between the knots is filled with a viscous substance with the dissipation
120 coefficient γ . The role of the viscous medium is important: We will demonstrate that
121 even a slow external excitation leads to intensive waves in the system, the energy
122 of these waves are eventually adsorbed by the viscosity. Without the viscosity, the
123 system never reaches a steady state.

124 The motion of the i th knot satisfies the equation

$$m_i \ddot{\mathbf{z}}_i + \gamma \dot{\mathbf{z}}_i = \sum_{j \in N(i)} \frac{F_{ij}(|\mathbf{z}_i - \mathbf{z}_j|)}{|\mathbf{z}_i - \mathbf{z}_j|} (\mathbf{z}_i - \mathbf{z}_j) \quad (11)$$

125 where \mathbf{z}_i is the vector of coordinates of i th knot, $|\cdot|$ is length of the vector, $N(i)$ is
126 the set of knots neighboring the knot i , m_i is the mass of the i th knot. The force F_{ij}
127 in the ij th link depends on the damage parameters $c_{ij,1}$ and $c_{ij,2}$ given in (10). The
128 set of neighboring knots depends on the geometric configuration.

129 *Remark 3.* In this model, the masses are permitted to travel as far as the elastic
130 links permit. Particularly, when these links are completely broken, the concentrated
131 mass moves “between” other masses without impact interaction with them.

132 Below in Section 4.4, we discuss a special model for the projectile that is “large
133 enough” and does not slip through the rows of linked masses.

134 2.3.1. *Setting*

135 The speed of waves in a structure is of the order of the speed of sound in the material
136 which the structure is made of (approximately 5000 m/s for steel). In our numerical
137 experiments, we assume that the speed of the impact is much smaller (recall that

the speed of sound in the air is 336 m/s). A slow-moving projectile does not excite
138 intensive waves in stable structures, but it does excite mighty waves of damage
139 in the waiting structure. The reason is that the energy stored in the elastic links
140 suddenly releases when the links are broken. This phenomenon explains the superb
141 resistance of the waiting structure: The energy of the projectile is spent to excite
142 the waves of damage.
143

2.4. NUMERICAL ALGORITHM 144

To solve the system (11) numerically, we first rewrite it as an autonomous system
145 of first-order differential equations:
146

$$\dot{\mathbf{z}}_i = \mathbf{p}_i, \quad (12)$$

$$\dot{\mathbf{p}}_i = \frac{1}{m_i}(\phi_i - \gamma \mathbf{p}_i) \quad (13)$$

where 147

$$\phi_i = \sum_{j \in N(i)} \frac{F_{ij}(|\mathbf{z}_i - \mathbf{z}_j|)}{|\mathbf{z}_i - \mathbf{z}_j|} (\mathbf{z}_i - \mathbf{z}_j). \quad (14)$$

Introducing the notation 148

$$\vec{\mathbf{x}} = \{\mathbf{z}_i, \mathbf{p}_i\}, \quad \vec{\mathbf{f}} = \left\{ \mathbf{p}_i, \frac{1}{m_i}(\phi_i - \gamma \mathbf{p}_i) \right\},$$

we get 149

$$\dot{\vec{\mathbf{x}}} = \vec{\mathbf{f}}(\vec{\mathbf{x}}).$$

We solve the resulting system via the second-order Runge–Kutta method

$$\vec{\mathbf{x}}_{n+1} = \vec{\mathbf{x}}_n + \frac{k}{2}(\vec{\mathbf{f}}(\vec{\mathbf{x}}_n) + \vec{\mathbf{f}}(\vec{\mathbf{x}}_n + h\vec{\mathbf{k}}(\vec{\mathbf{x}}_n))), \quad (15)$$

where k denotes the time step. Note that the stability condition of the resulting
150 method depends on the damage speed v_d from (7) and (9) and the dissipation
151 coefficient γ . In all numerical experiments that follow we establish convergence
152 empirically via time step refinement.
153

3. Damage of a Homogeneous Strip 154

We consider a homogeneous strip made as a triangular lattice with waiting links.
155 The left side of the strip is fixed while the right one is pulled with a given constant
156 speed V .
157

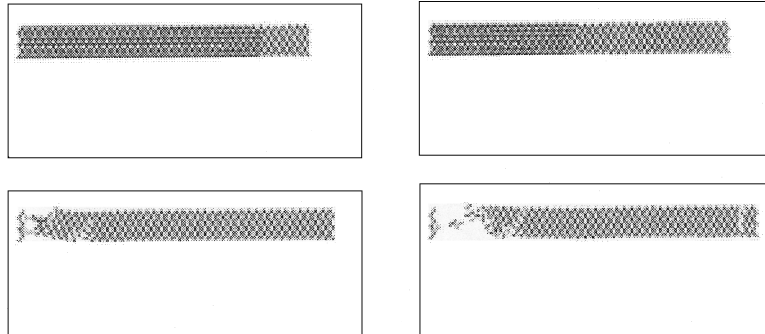


Figure 2. Evolution of damage in a fastly pulled lattice with waiting elements ($\alpha = 25\%$).

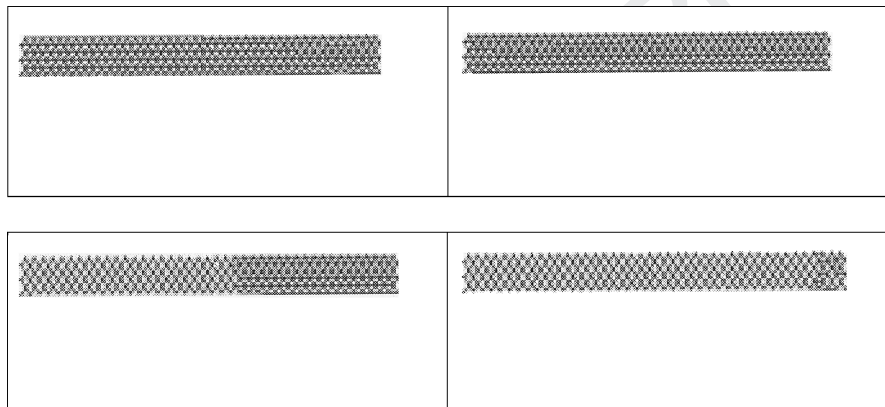


Figure 3. Evolution of damage in a slowly pulled lattice with waiting elements ($\alpha = 25\%$).

158 The next three figures show the comparison of damage evolution in the waiting
 159 link structures (Figures 2 and 3; $\alpha = 0.25$) and the structure from conventional
 160 brittle-elastic materials (Figure 4; $\alpha = 1.0$). Intact waiting links (both rods are
 161 undamaged) are shown by bold lines; partially damaged links (the shorter rod is
 162 destroyed, the longer one is undamaged) correspond to dashed lines; destroyed
 163 links (both links are damaged) are not shown.

164 Figures 2 and 3 illustrate an interesting phenomenon: controllability of the wave
 165 of damage. If the speed V is high, the wave of “partial breakage” (colored gray)
 166 propagates starting from the point of impact; when the wave reaches the other end
 167 of the chain, it reflects and the magnitude of stress increases; at this point, the
 168 chain breaks. Notice that the breakage occurs in the opposite to the impact end of
 169 the chain. If the speed is smaller, the linear elastic wave propagates instead of the
 170 wave of partial damage; the propagation starts at the point of impact. When this
 171 wave reaches the opposite end of the strip and reflects, it initiates a wave of partial
 172 damage that propagates toward the point of impact. Later, the strip will break near
 173 the point of impact (not shown).

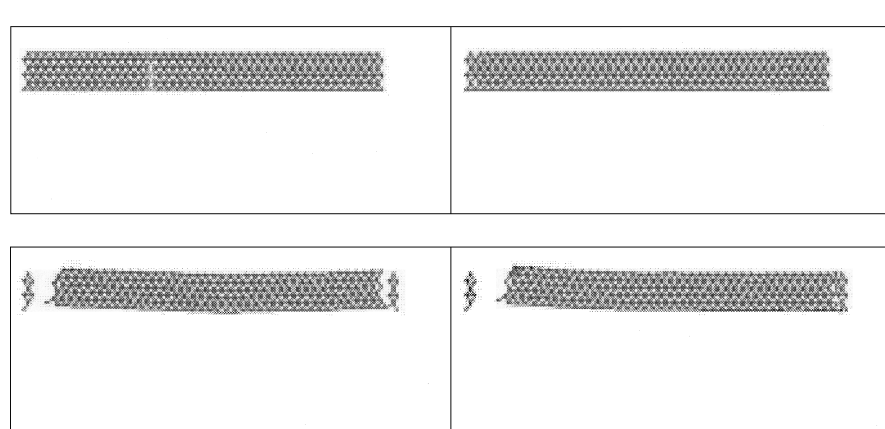


Figure 4. Evolution of damage in a slowly pulled lattice without waiting elements ($\alpha = 1$).

Figures 3 and 4 compare the waiting link structures with conventional brittle-
elastic structures (with the same pulling speed V and final time). One can see that
the conventional strip breaks near the point of impact as well as near the fixed side.
Note that only several links in the conventional structure break while all others stay
undamaged. To the contrary, the waiting link structure spreads “partial damage”
through the whole region, thereby dissipating the energy of the impact. As a result,
the waiting link strip preserves the structural integrity due to absorbing the kinetic
energy of the pulling.

Remark 4. The direct comparison of conventional and waiting link structures is
not easy: the energy dissipated in a conventional structure is proportional to its
cross-section (Figure 4) while the energy dissipated in the waiting link structure is
proportional to its volume (Figure 3).

4. Structures Under a Concentrated Impact

In this section, we investigate the resistance and failure of structures from waiting
links impacted by a massive concentrated projectile. The kinetic energy of the
projectile must be absorbed in the structure without its total failure.

4.1. MODEL OF THE PROJECTILE

Modeling the projectile, one needs to take into account the penetration of it through
the structure, and prevent it from slipping through the line of knots. Therefore one
cannot model the projectile as another “heavy knot” in the structure with an initial
kinetic energy: Such a model would lead to the failure of the immediate neighbor
links after which the projectile slips through the net without interaction with other
knots.

197 In our experiments, the projectile is modeled as an “elastic ball” of the mass M_p
 198 centered at the position z_p . Motion of the mass satisfies the equation

$$M_p \ddot{\mathbf{z}_p} = \sum_j \frac{F_{pj}(|\mathbf{z}_p - \mathbf{z}_j|)}{|\mathbf{z}_p - \mathbf{z}_j|} (\mathbf{z}_p - \mathbf{z}_j) \quad (16)$$

199 similar to (11), but the force F_{pj} is found from the equation

$$F_{pj}(z) = \begin{cases} 0 & \text{if } z > B \\ \ln\left(\frac{B-A}{z-A}\right) & \text{if } A < z \leq B \\ +\infty & \text{if } z \leq A \end{cases} \quad (17)$$

200 In the numerical experiments that follow we set $A = 0.5L$, $B = 2L$.

201 This model states that a repulsive force is applied to the knots when the distance
 202 between them and \mathbf{z}_p is smaller than a threshold B . This force grows when the
 203 distance decreases and becomes infinite when the distance is smaller than A . This
 204 model roughly corresponds to the projectile in the form of a nonlinearly elastic ball
 205 with a rigid nucleus. When it slips through the structure, the masses in the knots
 206 are repulsed from its path causing deformation and breaks of the links.

207 4.2. EFFECTIVENESS OF A DESIGN

208 Comparing the history of damage of several designs, we need to work out a quan-
 209 titative criterion of the effectiveness of the structure. This task is nontrivial, since
 210 different designs are differently damaged after the collision.

211 4.2.1. *Effectiveness Criterion*

212 We suggest an integral criterion that is not sensitive to the details of the damage;
 213 instead, we are measuring the variation of the impulse of the projectile. It is assumed
 214 here that the projectile hits the structure flying into it vertically down.

215 To evaluate the effectiveness, we compute the ratio R in the vertical component
 216 $p_v : \mathbf{p}_P = [p_n, p_v]^T$ of the impulse \mathbf{p}_P of the projectile before and after the impact:

$$R = \frac{p_v(T_{\text{final}})}{|p_v(T_0)|} \quad (18)$$

217 where T_0 and T_{final} are the initial and the final moments of the observation, re-
 218 spectively. The variation of impulse of the projectile R shows how much of it is
 219 transformed to the motion of structural elements. Parameter R evaluates the struc-
 220 ture’s performance using the projectile as the measuring device without considering
 221 the energy dissipated in each element of the structure; it does not vary when the
 222 projectile is not in contact with the structure.

223 Different values of the effectiveness parameter are presented in the Table I. An
 224 absolute elastic impact corresponds to the final impulse opposite to the initial one;

Table I. Effectiveness parameter R .

Effect	Range of R
Elastic contact with a rigid plane	−1
Projectile is rejected	(−1, 0)
Plastic contact (the projectile stops)	0
Projectile breaks through	(0, 1)
No effect	1

therefore in this case $R = -1$. The absence of the structure corresponds to $R = 1$, 225 because the impulse of the projectile does not change. If the projectile stops then 226 $d = 0$; if it breaks through the structure; then $R \in (0, 1]$; and if it is rejected, then 227 $R \in [-1, 0)$. The smaller the R is, the more effective the structure is. 228

4.2.2. Other Criteria 229

Other criteria compare the state of the structure before and after the collision. These 230 criteria are applicable only if the structure (or its pieces) reach a steady state after 231 the collision. This is why we need the dissipation factor in the model. Without this 232 factor, the elastic waves never stop and their interferences may cause additional 233 damage to the structure any time after the collision. 234

We register two criteria: 235

1. The percentage of partially damaged links. 236
2. The percentage of destroyed links. 237

The first number shows how effective the damage is spread, and the second shows 238 how badly the structure is damaged. Ideally, we wish to have a structure in which 239 all elements are partially damaged, but no element is completely destroyed. 240

Remark 5. The number of destroyed elements is a rough quality criterion. It ig- 241 nores a significant factor—the positions of the destroyed links. 242

4.3. BRIDGE-LIKE DESIGNS 243

Figures 5 and 6 show the dynamics of the damage of a bridge-like truss structure 244 made from waiting links (1). The structure is supported by its vertical sides. The 245 horizontal sides are free. It is impacted by a projectile that is modeled as an “elastic 246 ball” accordingly to Section 4.1. The projectile impacts the center of the upper side 247 of the structure moving vertically down with an initial speed v_0 . If the speed is 248 small, the projectile is rejected, otherwise it penetrates through the structure. 249

We simulate the damage process of the bridge by varying the parameter α (the 250 fraction of material put into the shorter link) while keeping the other parameters 251 ($L, \Delta, z_{f_1}, z_{f_2}$, total amount of material, etc.) the same for all runs. The results of the 252

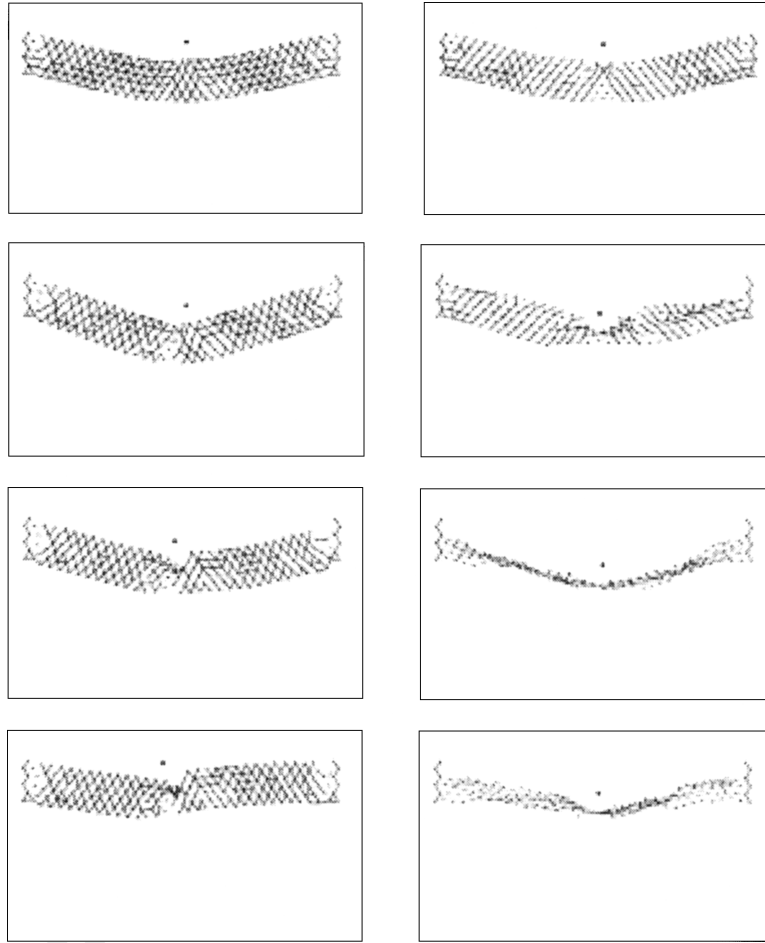


Figure 5. Evolution of damage in a lattice with waiting elements (left column $\alpha = 25\%$, right, column: $\alpha = 10\%$).

simulation are summarized in Table II. One can see from Table II that as α decreases from 1.00 (conventional structure) to 0.10 the percentage of partially damaged links increases as the percentage of destroyed links decreases making the structure more resistant. Table II also shows that $\alpha = 0.25$ is optimal for both minimizing the number of destroyed links and minimizing the effectiveness parameter R (see the discussion in Section 4.2).

The structures with $\alpha = 0.50$ and $\alpha = 1.00$ (conventional structure) soon develop cracks and fall apart allowing the projectile to go through (see Figure 6) while the structures with $\alpha = 0.10$ and $\alpha = 0.25$ preserve the *structural integrity* by dissipating energy and taking the stress away from the point of impact; this results in the rejection of the projectile (see Figure 5). Notice that the final time T_{final} is twice as small in the last two examples.

12

A. CHERKAEV AND L. ZHORNITSKAYA

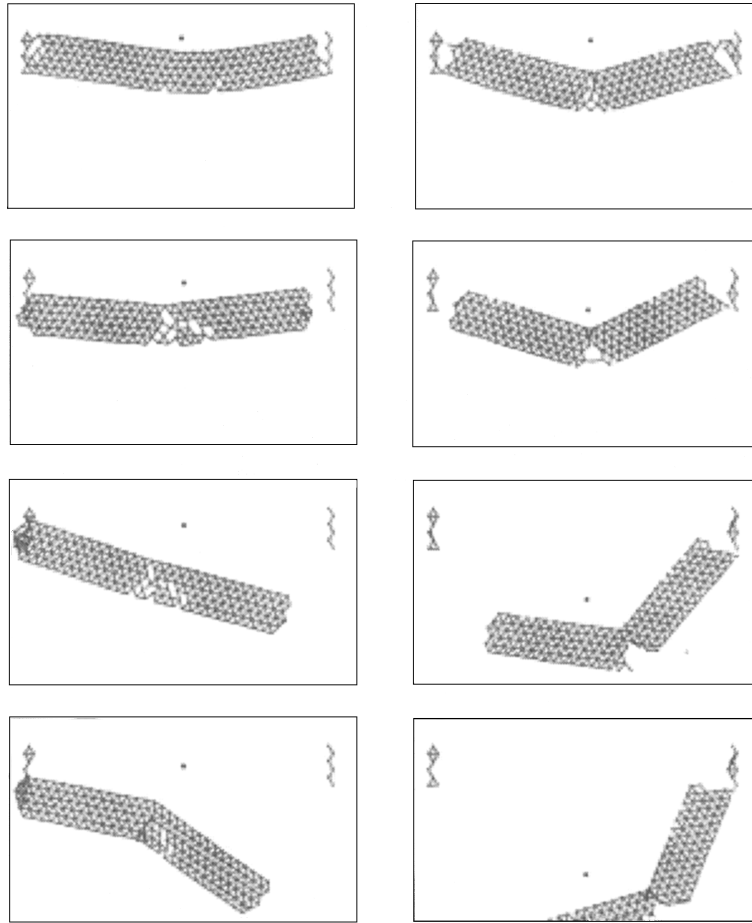


Figure 6. Evolution of damage in a lattice with (right, $\alpha = 50\%$) and without (left, $\alpha = 100\%$) waiting elements.

The propagation of the damage is due to several factors: the local instabilities of the part of the network that contains a damaged link; the force acting on neighboring links significantly increases and the damage spreads: the waves that propagate through the network and initiate the damage in the remote from the collision point areas.

4.4. DAMAGE OF A MASSIVE STRUCTURE

The following section describes the result of simulation of damage/destruction of network made from the waiting links and compares these structures with the nets from conventional links.

This series of experiments aims to show the wave of damage and strains in a “large” domain (the block). The block is supported from the sides, the bottom is

Table II. Damage and/or destruction of a bridge.

Figure	α	% of damaged links	% of destroyed links	Effectiveness R	Final time T_{final}
Figure 5 (right)	0.10	94	3.8	-0.26	500
Figure 5 (left)	0.25	42	3.8	-0.32	500
Figure 6 (right)	0.50	4.6	6.3	0.54	250
Figure 6 (left)	1.00	0	8.6	0.46	250

276 free (see Figure 7). As in the above mentioned simulations of the bridges, the block
 277 is impacted by a projectile that is modeled as an “elastic ball”. It is assumed that the
 278 projectile hits the center of the upper side of the structure moving vertically down
 279 with an initial speed v_0 .

280 Figure 7 demonstrates propagation of the elastic waves and the waves of partial
 281 and total damage of elements of the block. The conventional link structure soon
 282 develops cracks and gets destroyed, while the waiting link structure preserves its
 283 structural integrity. Notice that the damage is concentrated in conventional design
 284 and spread in the waiting link design.

285 5. Discussion

286 5.1. RESUME

- 287 1. Our numerical experiments have demonstrated the possibility of control of the
 288 damage process: Waiting links allow to increase the resistivity, increase the time
 289 of rupture, increase the absorbed energy, and decrease the level of concentration
 290 of damage.
- 291 2. The results emphasize the necessity of dynamics simulation versus computation
 292 of the quasi-static equilibrium: one can see from Figure 7 that damage can start
 293 in parts of the structure distant from the zone of impact. Development of damage
 294 is caused by excited waves and local instabilities.
- 295 3. We observe that the results strongly depend on parameters of the structure and
 296 projectile.

297 5.2. CONTINUUM AND DISCRETE MODEL

298 We use a discrete model of the structure rather than the continuous model for several
 299 reasons. First, it models the structures that can be made as we described. However,
 300 one may ask how to simplify the computation of the dynamics using a homogenized
 301 description of the networks. The process of damage is similar to the process of phase
 302 transition, since the initial (undamaged) phase is replaced by the partially damaged
 303 state and then by the destroyed state of structure in a small scale; such processes
 304 can also be described as a phase transition in solids, see for example [9].

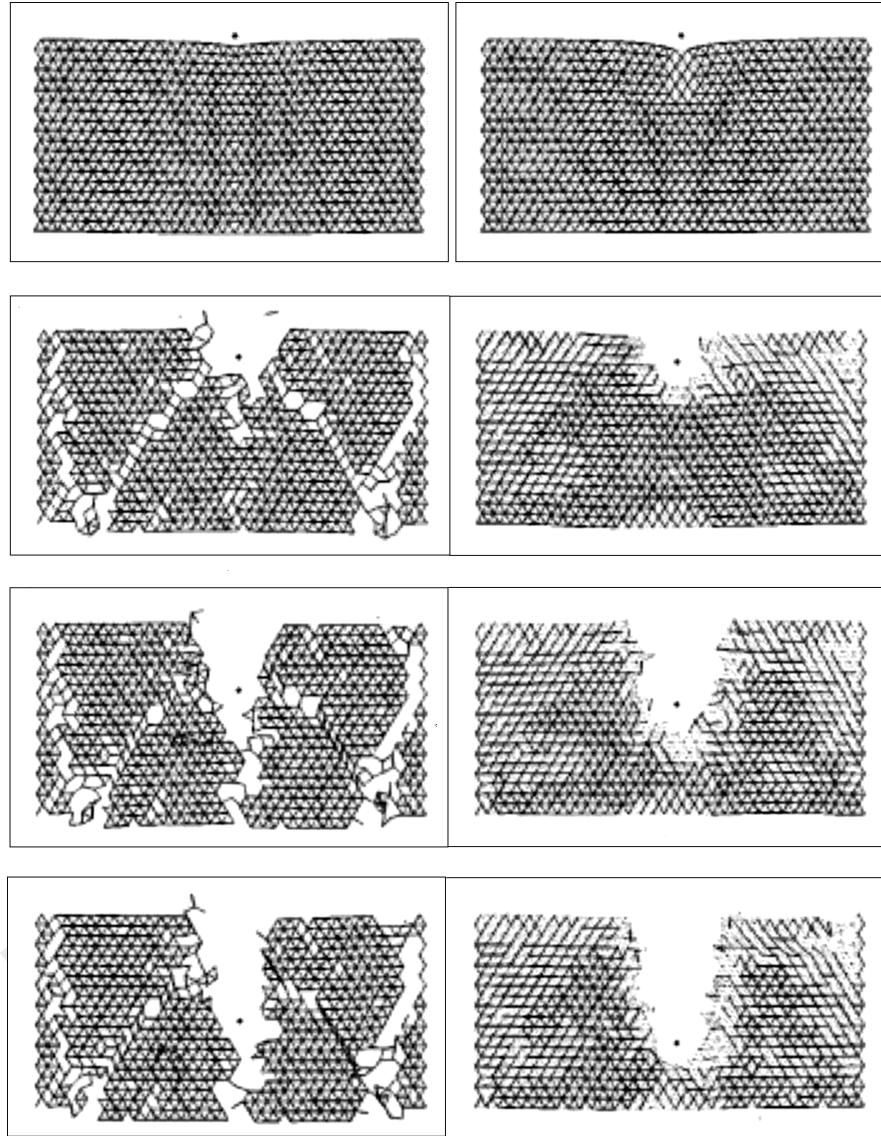


Figure 7. Evolution of damage in a lattice with waiting elements. Left field: lattice from elastic-brittle material; right field: lattice from waiting links, $\alpha = 0.25$.

The observed process is also significantly controlled by intensive waves caused by vibration of individual masses. The fast-oscillating motion carries significant energy and it is responsible for initiation of the damage in the parts of the structure that are not connected to the zone of impact, but are close to reflecting boundaries. In the continuum model, these oscillations would disappear and it is still unclear how to account for this energy in the homogenized model.

311 5.3. OPTIMIZATION

312 The demonstrated structures show the ability to significantly increase the resistance
 313 comparing with conventional materials. However, these results are still far away
 314 from the limit that can be achieved by optimizing the response by new design
 315 variables: The ratio α and the additional (slack) length ($\Delta - L$) of the waiting rod. In
 316 principle, these parameters can be separately assigned to each link, keeping the total
 317 amount of material fixed. However, there are natural requirements of robustness:
 318 A structure should equally well resist all projectiles independently of the point of
 319 impact, and should well resist projectiles approaching with various speed. Such
 320 considerations decrease the number of controls; it is natural to assign the same
 321 values of the design parameters to all elements in the same level of the structure.

322 One may minimize the absorbed energy, restricting the weight, admissible elongation,
 323 and the threshold after which the damage starts. In addition, one needs to
 324 restrict the range of parameters of a projectile: its mass, direction, and speed. The
 325 range of parameters is important: because of strong nonlinearity, the qualitative
 326 results are expected to be sensitive to them. The optimization problem is com-
 327 putationally very intensive since the dependence of parameters is not necessarily
 328 smooth or even continuous. We plan to address the optimization problem in the
 329 future research.

330 **Acknowledgment**

331 This work was supported by ARO and NSF.

332 **References**

- 333 1. Cherkaev, A. and Slepian, L., ‘Waiting element structures and stability under extension’, *International Journal of Damage Mechanics* **4**(1), 1995, 58–82.
- 334 2. Francfort, G.A. and Marigo, J.-J., ‘Stable damage evolution in a brittle continuous medium’, *European Journal of Mechanics A: Solids* **12**(2), 1993, 149–189.
- 335 3. Timoshenko, S.P. and Goodier, J.N., *Theory of Elasticity*, 2nd edn. McGraw-Hill Book Company, Inc., New York, Toronto, London, 1951.
- 336 4. Slepian, L.I., *Models and Phenomena in Fracture Mechanics*, Springer-Verlag, 2002.
- 337 5. Balk, A., Cherkaev, A. and Slepian, L., ‘Dynamics of chains with non-monotone stress-strain relations. I. Model and numerical experiments’, *Journal of Mechanics, Physics and Solids* **49**, 2001, 131–148.
- 338 6. Balk, A., Cherkaev, A. and Slepian, L., ‘Dynamics of chains with non-monotone stress-strain relations. II. Nonlinear waves and wave of phase transition’, *Journal of Mechanics, Physics and Solids* **49**, 2001, 149–171.
- 339 7. Slepian, L.I. and Ayzenberg-Stepanenko, M.V., ‘Some surprising phenomena in weak-bond fracture of a triangular lattice’, *Journal of Mechanics, Physics and Solids* **50**(8), 2002, 1591–1625.
- 340 8. Kyriafides, Stelios, ‘Propagating instabilities in structures’, *Advances in Applied Mechanics* **30**, 1994, 68–186.
- 341 9. Nekorkin, V.I. and Velarde, M.G., *Synergetic Phenomena in Active Lattices*, Springer-Verlag, 2002.
- 342 10. Morikazu, Toda, *Theory of Nonlinear Lattices*, Springer-Verlag, 1989.